mathematics

MDPI

Article

Inerter-Based Eigenvector Orientation Approach for Passive Control of Supersonic Panel Flutter

Pedro May †, Haitao Li † and Henry T. Yang *

Department of Mechanical Engineering, Univeristy of California, Santa Barbara, CA 93117, USA; pedromay@ucsb.edu (P.M.)
* Correspondence: henry.yang@ucsb.edu
† These authors contributed equally to this work.

Abstract: Inspired by the mass amplification property of inerters, an inerter-based passive panel flutter control procedure is developed and proposed. Formulations of aeroelastic equations of motion are based on the use of a wide-beam (flat panel) element stiffness equation subjective to supersonic flow using piston theory. The onset of flutter is analyzed using an eigenvector orientation approach, which may provide the advantage of lead time while the angle between eigenvectors of the first two coalescing modes reduces towards zero. The mass amplification effect of inerters is described and incorporated into the aeroelastic equation of motion of the passive actuation system for the investigation of flutter control. To demonstrate the potential applicability and usefulness of the proposed formulation and procedure, two numerical examples with one and two inerters, respectively, to optimally control the flutter of the panel modeled by wide-beam elements are presented. The results of the numerical simulation of the present examples demonstrate that the present inerter-based method can offset the onset of flutter to a higher level of aerodynamic pressure by optimizing the effective mass ratios and locations of inerters. In addition, this paper demonstrates that fundamental modes may be playing a role when identifying the optimal location of the inerters. It appears that the placement of the inerters may be more effective in controlling flutter at the highest amplitude of the mode shape along the wide beam. The procedure developed in this study may be of use for practical application for passive panel flutter control.

Keywords: passive flutter control; eigenvector orientation; finite element; panel flutter; inerter

MSC: 37M05

Citation: May, P.; Li, H.; Yang, H.T. Inerter-Based Eigenvector Orientation Approach for Passive Control of Supersonic Panel Flutter. *Mathematics* **2023**, *11*, 1462. https://doi.org/10.3390/math11061462

Academic Editors: Gaohui Wang, Elena Benvenuti and Lihua Wang

Received: 29 September 2022
Revised: 9 March 2023
Accepted: 16 March 2023
Published: 17 March 2023

1. Introduction

Panel flutter is the self-excited dynamic oscillation of an aeroelastic structure, which is one of the most destructive causes of failure for various aircraft, including missiles, airplanes, and rockets. Flutter arises when the speed of an aircraft reaches a critical velocity under the coupling action of elastic force, inertia force, and aerodynamic pressure.

There have been various panel flutter modeling methods used to characterize and solve the aeroelastic problem of flutter. Among these methods, the aeroelastic model using the finite element method has gained widespread acceptance due to its flexibility in handling the geometry and boundary conditions of aeroelastic structures [1]. The earliest finite element model for flutter detection is the two-dimensional wide-beam element [2] and three-dimensional rectangular plate element [3] by Olson. According to the paper, flutter detection can be formulated as a set of eigenvalue equations in order to find the flutter speeds and mode shapes. The onset of flutter occurs during the coalescence between two eigenvalues. To track the response time depicted with a lead time, an alternative eigenvector orientation method was developed by the current senior author to predict the onset of flutter [4–6]. In this study, the eigenvector orientation-based method will be used to detect panel flutter.

In order to control panel flutter, an active controlling method using smart material is widely adopted. Piezoelectric material is one of these smart materials due to its excellent electromechanical characteristics [7]. In recent years, different types of models, controlling strategies, and applications of piezoelectric actuators have been studied [8–10]. A common strategy used to solve flutter problems involves offsetting the critical velocity corresponding to panel flutter to a higher level. For example, Forster and Yang built a six-bay wing box model using finite elements and examined the use of piezoelectric actuators to control the supersonic flutter of the wing box aeroelastic models [11]. Subsequently, Wang and Yang developed a panel flutter suppression strategy using piezoelectric actuators. The use of the eigenvector orientation method has the potential to provide a lead time for flutter control [4].

For passive flutter suppression, mass balancing is one method often used by aircraft designers. Through the distribution of the structure mass, a higher critical velocity can be obtained. Thus, the concept of using an inerter, which was first presented by Smith et al. [12,13], could be attractive for passive flutter suppression. It can develop a reaction force proportional to the relative acceleration and generate an effect of mass amplification. As a mass amplifier with a small physical mass, an inerter has been successfully applied to the vibration control of various systems, including automobile suspension [14], train suspension [15–18], motorcycle steering [19,20], buildings [21], and more. In a recent paper by the current authors, Li, Yang, et al. used six earthquake data to show the effectiveness of a bio-inspired passive base isolator with a tuned mass damper inerter for structural control [22]. Meanwhile, a ball-screw inerter [23], hydraulic inerter [24], and other varieties of inerters are introduced in addition to the original fly-wheel inerter. The applications show that an inerter can improve the vibration performance of structures. In light of the performance benefits of inerters, this study aims at exploring their effectiveness while being used as a passive actuator for flutter suppression.

The purpose of this study is to focus on the passive control of panel flutter using the concept of inerters to formulate the aeroelastic equations, while also using the eigenvector orientation method to solve them in order to take advantage of tracking the response time with a possible lead time before the occurrence of flutter. In order to illustrate this concept, and to investigate its feasibility for applications, a simple illustrative example of a two-dimensional panel (a wide beam) is chosen, similar to Olsen [2]. Furthermore, two inerters are chosen as a specific example. For the specific examples chosen, the present proposed procedure and numerical results have demonstrated that optimum effectiveness in passive flutter control can be achieved by installing one or two inerters, respectively.

The formulation of an aeroelastic model for the wide-beam panel flutter is described in Section 2. Based on the equation of motion with the inerter of the aeroelastic panel in Section 3, the angle between two coalescing eigenvectors can be calculated. The angle will gradually decrease to zero when flutter arises. Section 4 presents the design of the control strategy. The location and effective mass ratio of the inerter are two crucial parameters that influence the control effect. By optimizing the location and effective mass ratio, the optimal results can be obtained for an aeroelastic structure installed with one and two inerters. Numerical simulation with various examples of a simply supported wide-beam panel for flutter control has been analyzed, with results evaluated numerically and interpreted physically using the eigenvalue or eigenvector orientation method, in Section 5. It is of interest to observe that the optimal locations of the inerter may be correlated with the fundamental mode shape of a simply supported wide-beam panel.

2. Formulations of Panel Flutter

2.1. Identification of Flutter

Flutter is an instability encountered in aircraft and other aeroelastic structures subjected to fluid flow. It is the result of interactions between aerodynamics, stiffness, and inertial forces. When the flow speed of the fluid increases to a critical point, the structural damping of an aircraft will be insufficient to dampen out the motion due to aerodynamic

forces acting on the structure. At this point, the net damping, which is described as the sum of the structure's natural positive damping and negative damping of aerodynamic forces, goes to zero, and the structure is in a simple harmonic motion. Flutter will then occur if there is any other further decrease in net damping. Usually, the amplitude of flutter increases exponentially with time for a linear system, although it is limited for nonlinear structural systems [25,26].

The skin panel of a flying vehicle can simply be depicted as in Figure 1. It can be seen that airflow only acts on one surface of the panel on a two-dimensional simply supported wide beam. High-speed airflow may cause the skin panel of a flying vehicle to vibrate transversely with high amplitudes, which can be characterized as in Figure 1. As the speed of an aircraft increases, the frequencies of the two lowest modes may coalesce to create one mode, and thus flutter is initiated. If the flutter-induced stress level exceeds the yield stress of the structure, failure will occur. On the other hand, when subjected to a relatively low stress level but for a long period, the structure can also experience fatigue problems [26].

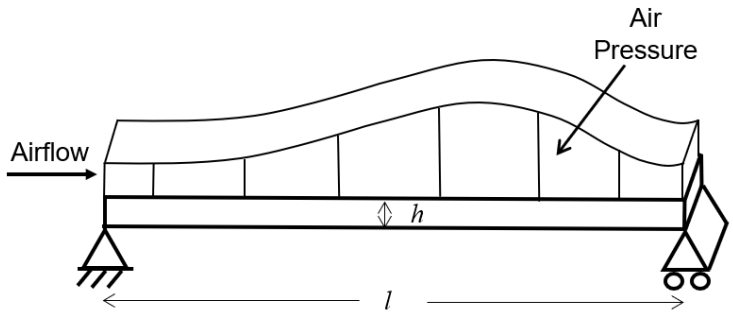

Figure 1. Three-dimensional sketch of panel flutter.

The occurrence of panel flutter can be influenced by various factors, including the mass, damping, and stiffness of the panel; local Mach number; dynamic pressure; density, and boundary conditions [26]. To avoid flutter, an aircraft is designed with the capability to predict the natural parameters and aerodynamic parameters, including flutter speed.

2.2. An Illustrative Example of an Aeroelastic Model of Panel Flutter

The panel is assumed to be a thin, stress-free plate with thickness h, length l, width s, and mass density per unit volume ρ. Only two-dimensional deformation of the panel is considered, which is described in Figure 1. A supersonic airstream flows over the upper surface, and the lower surface of the panel is not exposed to any airflow. The effect of air entrapped below the panel is also neglected. The aerodynamic pressure for Mach numbers $M_\infty > 1.7$ can be calculated with good accuracy through first-order piston theory [27]. Assuming a first-order, high Mach number approximation to the linear piston theory, the aerodynamic pressure acting on one surface is given as follows [5,28]:

$$p = \frac{2q_f}{\sqrt{M_\infty^2 - 1}}\left(\frac{\partial}{\partial x} + \frac{1}{U}\frac{M_\infty^2 - 2}{M_\infty^2 - 1}\frac{\partial}{\partial t}\right)\omega \tag{1}$$

In Equation (1), q_f is the free stream dynamic pressure, M_∞ is the Mach number, and U is the flow velocity. The dimensional aerodynamic pressure parameter A can be described as follows according to the above equation:

$$A = \frac{2q_f}{\sqrt{M_\infty^2 - 1}} \tag{2}$$

D is the bending rigidity of the aeroelastic structure and can be expressed using the following equation [29]:

$$D = \frac{Eh^3}{12(1-v^2)} \tag{3}$$

where E is the modulus of elasticity and v is the Poisson ratio.

3. Flutter Controlling Model with Inerter

3.1. Equation of Motion of Inerter

The ideal inerter is a two-terminal mechanical device that has the property that equal and opposite forces applied at two terminals are proportional to the relative acceleration between nodes [12,13]. Now, various physical models of an inerter have been proposed by researchers. The most widely known model is one that incorporates a rack-and-pinion to transform the translational kinetic energy associated with the relative motion of the device terminals into rotational kinetic energy at a lightweight fast-spinning "flywheel" [12,13]. The inertance of such a flywheel-based inerter depends primarily on the number of gears and the gear ratio used to drive the flywheels, rather than on the mass of the flywheels. A schematic representation of the inerter device is presented as a hatched box in Figure 2 [13].

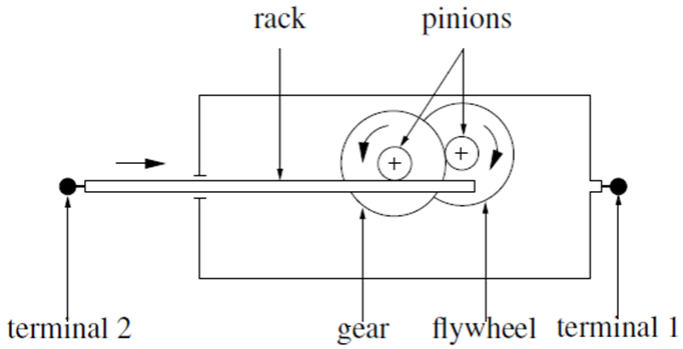

Figure 2. Schematic representation of the two-terminal inerter [13].

Assuming that the physical mass of the inerter is negligible compared to the mass of the structure, the force F of an ideal linear inerter would be proportional to the relative acceleration of its terminals, as described in the following equation [13].

$$F = b(\ddot{z}_1 - \ddot{z}_2) \tag{4}$$

In Equation (4), the constant b is the inertance measured in mass units (kg), where $\ddot{z}_1$ and $\ddot{z}_2$ are accelerations between two terminals of the inerter.

3.2. Aeroelastic Equation of Motion of Structure with Inerter

The aeroelastic structure can be modeled using a simply supported wide beam, which can be spatially discretized by wide-beam elements. The element has two nodes (joints) and four degrees of freedom. For each node, there are two degrees of freedom (DOF), including a transverse deflection v and an angle of rotation θ. The transverse shear force and bending moment corresponding to v and θ of two nodal points of the element can be expressed as $[Y_1 \ M_1 \ Y_2 \ M_2]$.

For a one-element wide-beam model of an aeroelastic structure installed with one inerter at each node, forces are applied in the inner surface of the structure that is not exposed to the airstream. The physical mass of an inerter is negligible relative to the structure mass, but the equivalent effect as the mass increases by b can be achieved by installing an inerter with inertance b. Thus, flutter control can be realized by using an inerter through modifying the structural mass matrix.

Similar to the lumped mass at nodal points, there is no bending moment created by an inerter. The transverse force of an inerter is proportional to the acceleration of the node, which can be described as follows:

$$Y_{ine} = b \cdot \ddot{v} \tag{5}$$

This study uses $U_{ine} = [Y_{1-ine} \;\; M_{1-ine} \;\; Y_{2-ine} \;\; M_{2-ine}]^T$ to represent the transverse force and rotational force exerted by the inerters installed at the two nodal points of an element for the simply supported wide beam. It can be expressed by the following equation:

$$U_{ine} = \begin{bmatrix} Y_{1-ine} \\ M_{1-ine} \\ Y_{2-ine} \\ M_{2-ine} \end{bmatrix} = \begin{bmatrix} b_1 & 0 & 0 & 0 \\ 0 & 0 & 0 & 0 \\ 0 & 0 & b_2 & 0 \\ 0 & 0 & 0 & 0 \end{bmatrix} \begin{bmatrix} \ddot{v}_1 \\ \ddot{\theta}_1 \\ \ddot{v}_2 \\ \ddot{\theta}_2 \end{bmatrix} \tag{6}$$

In Equation (6), b_1 and b_2 are the inertance of the inerters at two nodes of the element.

The simply supported wide beam can be modeled by n elements with the boundary condition that there is no transverse deflection for the two end nodes. According to the aeroelastic model of panel flutter and finite element theory [2], the equation of motion of the ith element can be described as follows:

$$(K + A_e)Q_i + M\ddot{Q}_i + B\ddot{Q}_i = U \tag{7}$$

K and A_e are the stiffness matrix and aerodynamic matrix, respectively [2,29]; M is the mass matrix [29] and B is the equivalent mass matrix exerted by the inerter, while Q_i represents the vector of joint displacements for two nodes of the element. U is the vector of external controlling forces implemented on the element.

$$K = \frac{D}{L^2} \begin{bmatrix} 12 & 6L & -12 & 6L \\ 6L & 4L^2 & -6L & 2L^2 \\ -12 & -6L & 12 & -6L \\ 6L & 2L^2 & -6L & 4L^2 \end{bmatrix} \tag{8}$$

$$A_e = A \cdot L \begin{bmatrix} -\frac{1}{2} & \frac{L}{10} & \frac{1}{2} & -\frac{L}{10} \\ -\frac{L}{10} & 0 & \frac{L}{10} & -\frac{L^2}{60} \\ -\frac{1}{2} & -\frac{L}{10} & \frac{1}{2} & \frac{L}{10} \\ \frac{L}{10} & \frac{L^2}{60} & -\frac{L}{10} & 0 \end{bmatrix} \tag{9}$$

$$M = \frac{\rho AL}{420} \begin{bmatrix} 156 & 22L & 54 & -13L \\ 22L & 4L^2 & 13L & -3L^2 \\ 54 & 13L & 156 & -22L \\ -13L & -3L^2 & -22L & 4L^2 \end{bmatrix} \tag{10}$$

$$B = \begin{bmatrix} b_1 & 0 & 0 & 0 \\ 0 & 0 & 0 & 0 \\ 0 & 0 & b_2 & 0 \\ 0 & 0 & 0 & 0 \end{bmatrix} \tag{11}$$

$$Q_i = \begin{bmatrix} v_1 & \theta_1 & v_2 & \theta_2 \end{bmatrix}^T \tag{12}$$

$$U = \begin{bmatrix} Y_1 & M_1 & Y_2 & M_2 \end{bmatrix}^T \tag{13}$$

The equation of motion of an element is based on the assumption that the damping of the aeroelastic structure is not taken into account in order to calculate the angles between eigenvectors [2]. It can be seen from the analysis and conclusions of Sun [30] that the aerodynamic damping of aeroelastic structures has little effect on the boundary of panel

flutter, even though it may affect the limit cycle deflection significantly. Moreover, the equation of motion of the aeroelastic structure can be obtained by assembling the above finite element matrices.

3.3. Eigenvector Orientation Approach for Flutter Detection

If there are no external controlling forces acting on the structure, U will become zero and then flutter can be transformed to a free vibration problem, which can be decoupled using the eigenvalue or eigenvector orientation method [30,31]. In flutter problems, the eigenvalues of different modes are usually distinct, and the eigenvectors generally satisfy the orthogonality condition if the structure is in stability, but, during flutter, two of the modes will approach each other and coalesce at a critical point. Then, the eigenvalues corresponding to the two modes become complex conjugate pairs, and the corresponding eigenvectors also lose their orthogonality gradually. To predict and control the onset of panel flutter, this study will adopt the eigenvector orientation approach by tracking the angle between two eigenvectors corresponding to the coalescing eigenvalue [4].

The angle between two eigenvectors can be derived from their scalar product. For two eigenvectors v_1 and v_1, it can be expressed by the arc-cosine. If the two eigenvectors are real, the angle can be obtained using Equation (14) [30],

$$\theta = cos^{-1}\left(\frac{v_1 \cdot v_2}{\|v_1\| \cdot \|v_2\|}\right) \tag{14}$$

If the two eigenvectors are complex, the angle can be obtained using Equation (15) by replacing one of the vectors with its complex conjugate [30],

$$\theta = cos^{-1}\left(\frac{\overline{v}_i \cdot v_j}{\|\overline{v}_i\| \cdot \|v_j\|}\right) \tag{15}$$

where the overbar denotes complex conjugation.

4. Design and Optimization of Control Strategy for the Illustrative Example

In this section, two different types of control strategies including one and two inerters are considered. The schematic diagram of the controlling model is shown in Figure 3. Given the number of inerters used for flutter control, the location and effective mass ratio will be optimized using a genetic algorithm [32].

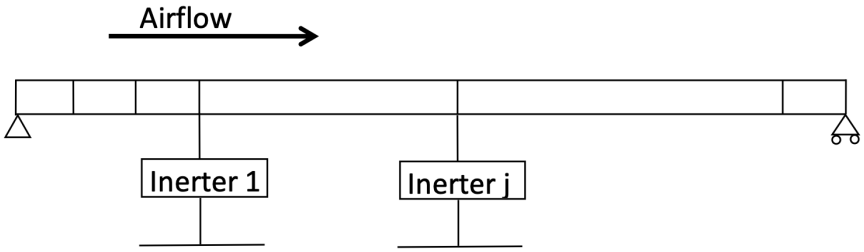

Figure 3. Schematic diagram of finite element model installed with inerters for flutter control.

For simplicity, the wide-beam example is discretized into eight and thirty-two 4-degrees-of-freedom beam elements in order to perform the feasibility study of the various numbers of inerters and various locations. One terminal of the inerter will be assumed to be connected to the wide beam and the other terminal will be connected to a fixed structure inside the wing.

4.1. Controlling Strategy with One Inerter

The strategy with one inerter is used to explore its effect on flutter control. It can be modeled as a nonlinear programming problem. The objective is to maximize the critical aerodynamic pressure parameter A_0 corresponding to the onset of flutter as seen in Equation (16):

$$maxA_0 = f(r_1, p_1) \tag{16}$$

where the design parameters r_1 and p_1 are the effective mass ratio and location of the inerter, respectively. The effective mass ratio of the inerter r_1 represents the ratio between the inertance of inerter b_1 and the mass of the structure m_s, which can be described using Equation (17):

$$r_i = \frac{b_i}{m_s} \tag{17}$$

Usually, the effective mass ratio will have an upper limit r. The location of the inerter can be described as $p = i$, which indicates that the inerter is placed at the ith joint for the finite element model. The side constraints are

$$\begin{cases} 0 < r_i < r \\ 0 < p_1 = i < n \end{cases} \tag{18}$$

It is noticed that the constraints described by the above equations define a multi-dimensional space of uncertain parameters. Through the application of the genetic algorithm [32], the optimal effective mass ratio and location of the inerter can be obtained. For the present flutter control model, the mass of the inerter is not taken into account because it is usually negligible relative to the relatively large mass of the aeroelastic structure.

4.2. Controlling Strategy with Multi-Inerter

It is of interest to investigate aeroelastic structures with multi-inerters in addition to the case of using a single inerter. In the controlling strategy of multi-inerters, the inerters are located at different locations and with different effective mass ratios. Given the number of inerters m, the optimization becomes a more complicated problem with more design parameters compared to the one-inerter strategy.

The objective function for assumed m inerters can be described as follows:

$$maxA_0 = f(\{r_1, p_1\}, \cdots, \{r_m, p_m\}) \tag{19}$$

The side constraints are

$$\begin{cases} 0 < r_i < r \\ 0 < p_1 < p_2 < \cdots < p_{m-1} < n \end{cases} \tag{20}$$

5. Numerical Simulation

In order to illustrate the proposed concept, formulations, and numerical solution methods as described in Sections 2 and 3, a simple illustrative example of a two-dimensional panel is chosen. Furthermore, one and two inerters located in different sections of the panel are chosen as specific examples. Although general conclusions may not be drawn, the example may reveal the feasibility, applicability, and advantages of the proposed method for the current examples chosen.

Various examples of a simply supported wide beam for panel flutter control have been analyzed, with results evaluated numerically and interpreted physically using the eigenvalue or eigenvector orientation method. The results show that these methods are effective in offsetting flutter to a higher level. To illustrate the formulation and computational procedures for flutter control, which have been discussed in the preceding sections, two different examples of a simply supported wide-beam panel installed with an inerter are considered. Two cases of flutter control with one and two inerters are presented, respectively. In particular, the optimal effective mass ratios and locations of the inerters are explored in order to obtain the best flutter control performance.

In this section, a Matlab program is developed to verify the present method as applied to supersonic panel flutter analysis. For simulation, the simply supported isotropic panel in the form of a wide beam is used. The panel's width, length, and thickness are 1 inch, 10 inches, and 0.1 inches, respectively. Material parameters of the isotropic beam, such as the modulus of elasticity, Poisson's ratio, and mass density, are assumed as E = 30 Mpsi, v = 0.3, and ρ = 0.1 lb/in^3, respectively. The aerodynamic pressure parameter defined in Section 2 will be used to characterize the property of flutter. The eigenvector orientation method is adopted to detect the critical aerodynamic pressure parameter and evaluate the control effectiveness of inerters under different configurations of effective mass ratios and locations.

5.1. Case 1—Flutter Control with One Inerter

For the aeroelastic structure without any controlling forces and bending moments, the variations in its two lowest coalescing natural frequencies and the angles between their corresponding eigenvectors are displayed in Figures 4 and 5, respectively. The figures show that flutter occurs at a critical point where the curves of two eigenvalues first coalesce and the angle between their corresponding eigenvectors approaches zero. At this point, the aerodynamic pressure parameter reaches a critical value A_0 = 314 psi. This paper will use the dimensional modified dynamic pressure parameter as seen in Figures 4 and 5. However, if Figures 4 and 5 are converted to the dimensionless modified dynamic pressure parameter, then it will result in an identical graph as seen in Olsen [3] and Sebastijanovic [6].

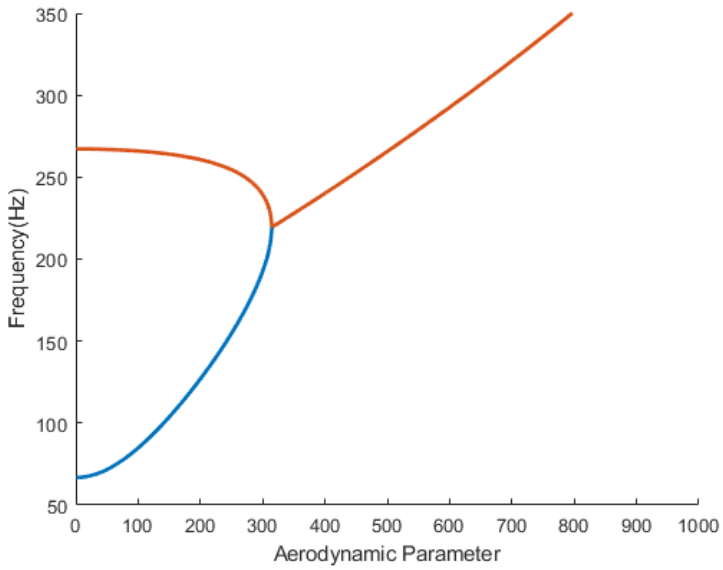

Figure 4. The coalescing of the two lowest natural frequencies of the wide beam without control.

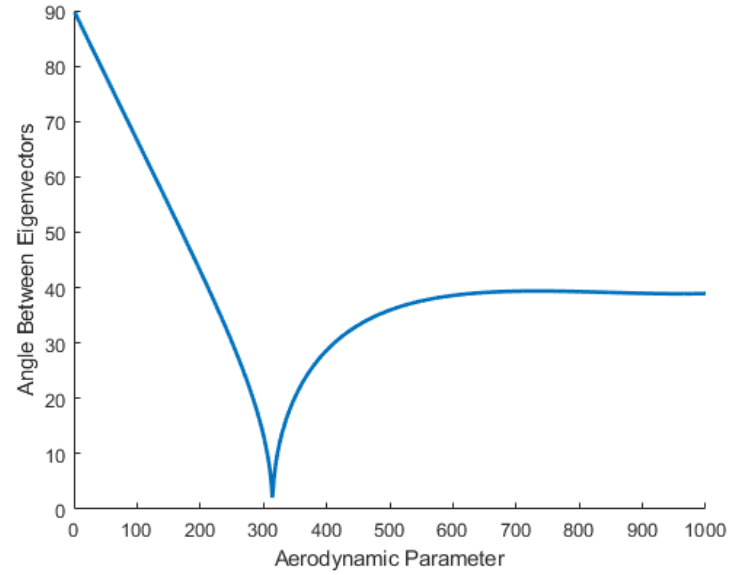

Figure 5. The variation in angle between two eigenvectors of the wide beam without control.

In order to investigate the property of the wide-beam panel installed with one inerter, the aerodynamic model with 8 elements is used. To demonstrate the effect of an inerter installed on the beam, the schematic diagram of the finite element model with the inerter installed at joint 3, 1/4 of the beam length, is shown in Figure 6. While holding the inerter at joint 3 and varying its effective mass ratio, the resulting aerodynamic pressures, obtained as the angles between the first two sets of eigenvectors become zero, are as shown in Figure 7. It can be observed that the inerters installed at joint 3 with increasing effective mass ratios can have different effectiveness for flutter control. Figure 8 shows the relationship between the effective mass ratio of the inerter and the critical aerodynamic pressure parameter corresponding to the onset of flutter. In Figure 8, the critical aerodynamic pressure parameter rises until reaching a critical point; at this point, the first two lowest modes no longer coalesce and coalescing occurs at higher modes. For the purpose of the present preliminary basic conceptual study, the focus is on the first two modes.

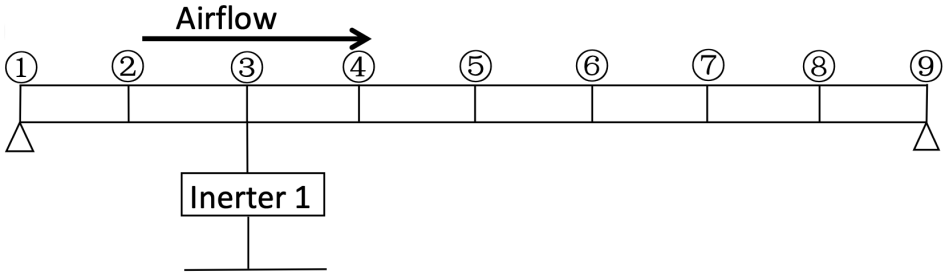

Figure 6. Schematic diagram of flutter control with one inerter installed at joint 3, out of 9 joints, for an 8-finite-element model.

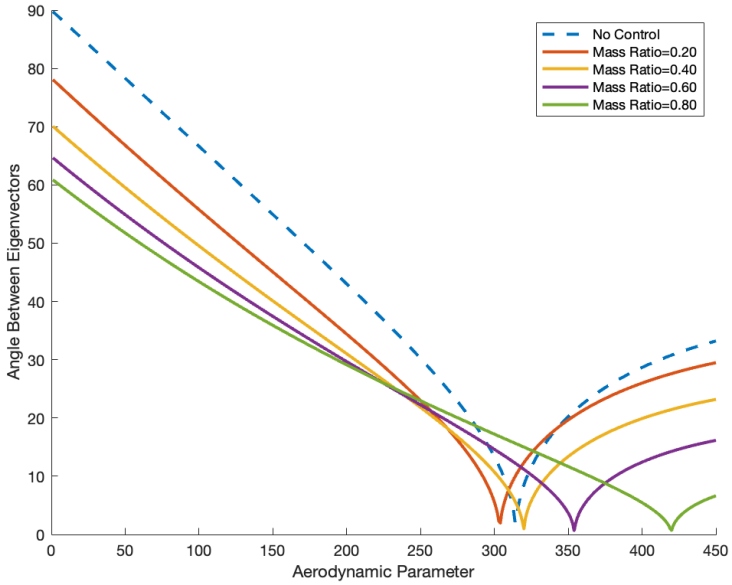

Figure 7. Angles between eigenvectors of the first two coalescing modes with different effective mass ratios of inerter applied at joint 3.

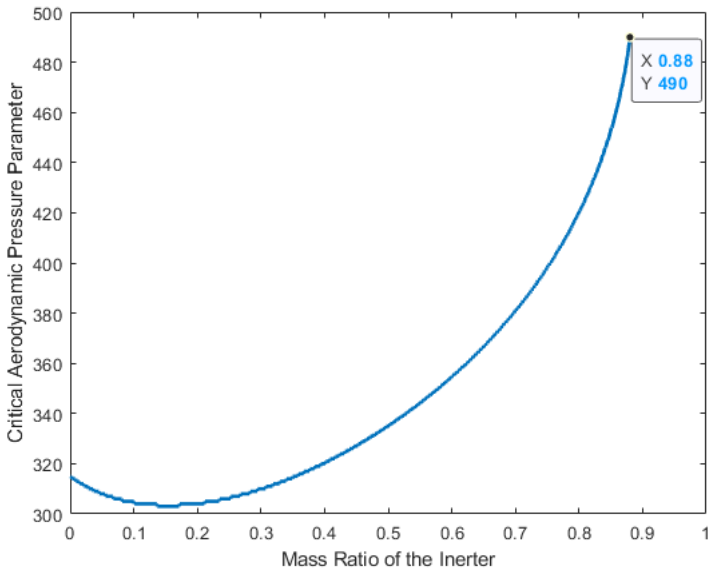

Figure 8. Critical aerodynamic pressure parameter corresponding to the onset of flutter with variable effective mass ratio.

To demonstrate the effectiveness of varying the location on an inerter for flutter control, an inerter is set to a constant of $r_1 = 0.39$. This value was chosen as a starting point for the iterative optimization process. After testing a range of starting points from 0 to 2, the optimization always converged to the same results; therefore, $r_1 = 0.39$ is used as a best guess starting point. The results for $r_1 = 0.39$ are shown in Figures 9 and 10.

These results suggest that there may be some optimal effective mass ratio and location of the inerter for flutter control. For inerters installed at different joints, the relationship between the critical aerodynamic pressure parameter and the effective mass ratio is presented in Figure 11. It is seen that the best control effectiveness can be obtained when the inerter is applied at the midspan location joint 5, 1/2 of the beam length.

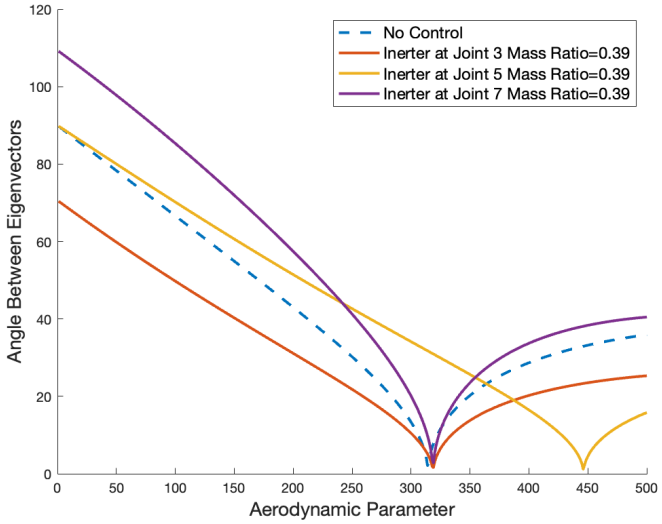

Figure 9. Angles between eigenvectors of two coalescing models with inerter placed at different joints.

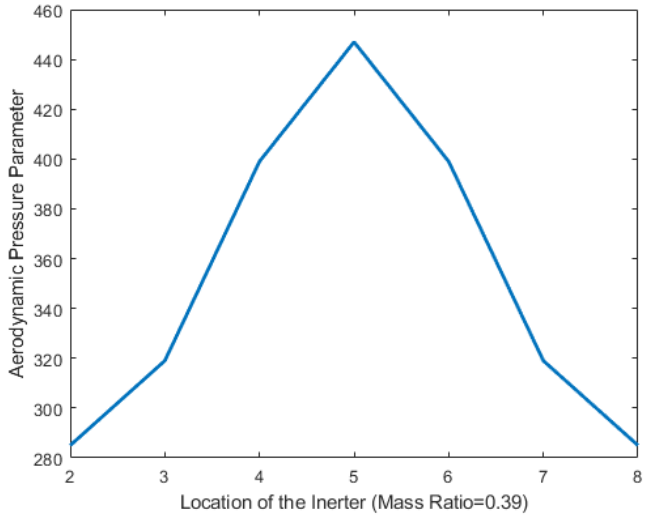

Figure 10. Critical aerodynamic pressure parameter corresponding to the onset of flutter with variable locations of inerter for effective mass ratio = 0.39.

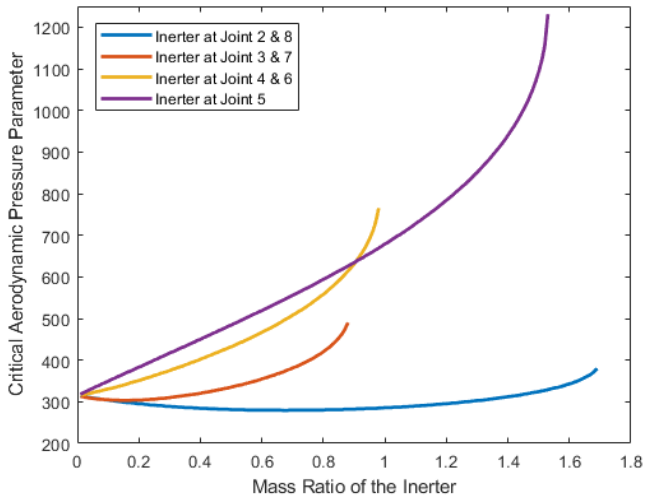

Figure 11. Critical aerodynamic pressure parameter for inerters applied at different joints of the 8-element model.

With variable effective mass ratios, the optimal critical aerodynamic parameter can be achieved for different locations of inerters. The optimized results are illustrated in Figure 12 with data given in Table 1. It can be noted that the peak critical aerodynamic pressure parameter 1231 can be achieved by using an inerter with an effective mass ratio of 1.53 located at the midspan joint 5. For this wide-beam panel model with both ends simply supported, it is seen that the effectiveness of flutter control can best be obtained when an inerter is installed in the midspan of the wide beam. It is interesting to observe that the critical aerodynamic pressure is shifted to the highest value of 1231 when the inerter is placed at the midspan of the beam panel, and the preferred joint locations are ranked as 5, 4 and 6, 3 and 7, and 2 and 8. Further increasing the effective mass ratio will cause the two lowest modes to no longer coalesce, and coalescing may occur at higher modes. However, for this study, only coalescing of the first two modes will be analyzed. From a practical viewpoint of engineering design, investigating coalescing above the first two lowest modes may be beyond the scope of the present basic conceptual study. It is of interest to note that while summarizing the results as shown in Figures 10 and 12, there seems to be a correlation between the first natural mode shape of a simply supported wide-beam panel and the optimal placement of inerters. Thus, the mode shape of the lowest natural frequency may serve as a reference basis for the placement of the inerter.

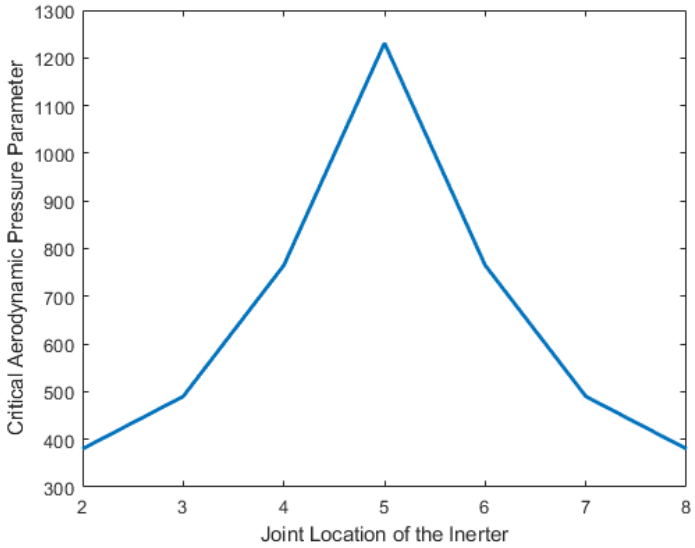

Figure 12. The peak critical aerodynamic pressure parameter for inerters installed at different joints of the 8-element model.

Table 1. Optimal design parameter configuration of inerters installed at different locations.

Location of Inerter (Joint Number)	Without Control	2	3	4	5	6	7	8
Optimal Effective Mass Ratio	/	1.69	0.88	0.98	1.53	0.98	0.88	1.69
Critical Aerodynamic Pressure Parameter	315	380	460	765	1231	765	490	380

The peak critical aerodynamic pressure parameter for inerters installed at different locations can be observed in Figure 13. It is observed that the effectiveness of flutter control can best be obtained when the inerter is installed at joint 16, 1/2 of the beam length, which is the midspan.

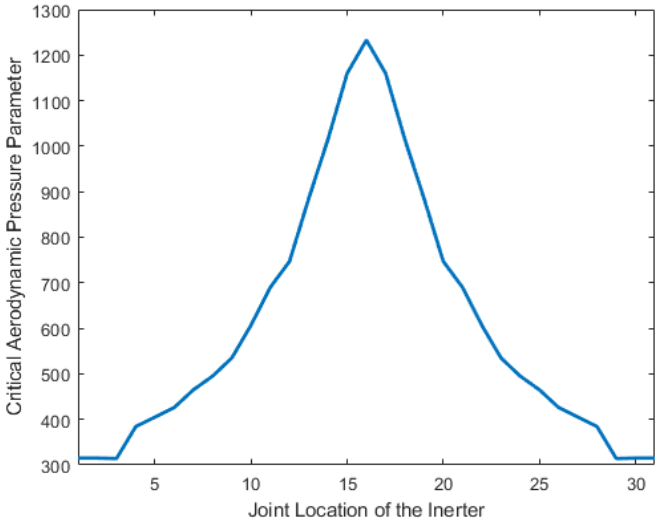

Figure 13. The peak critical aerodynamic pressure parameter for inerters installed at different locations (32-element model).

5.2. Case 2—Flutter Control with Two Inerters

To further explore the flutter control effectiveness, examples of flutter control with two inerters are considered.

5.2.1. Two Inerters Installed at Joints 3 and 5 with Varying Effective Mass Ratios

By changing the locations and the effective mass ratios of inerters, different control effects can be obtained. The first case of two inerters is shown in Figure 14, where two inerters are installed at joints 3, 1/4 of the beam length, and 5, 1/2 of the beam length. If the effective mass ratios of the inerters range from 0 to 2.0, it can be seen that the peak critical aerodynamic pressure parameter with a value of 1236 can be obtained, while the effective mass ratios of inerter 1 and inerter 2 are 0.09 and 1.89, respectively. For some of the configurations of the effective mass ratio, critical aerodynamic parameters corresponding to the onset of flutter are as listed in Table 2.

Table 2. Critical aerodynamic pressure parameter for some effective mass ratio configurations of 2 inerters installed at joints 3 and 5.

	1	**2**	**3**	**4**
Effective Mass Ratio of Inerter Installed at Joint 3	0.09	0.09	0.09	0.09
Effective Mass Ratio of Inerter Installed at Joint 5	0.50	1.00	1.50	1.89
Critical Aerodynamic Pressure Parameter	446	596	796	1236

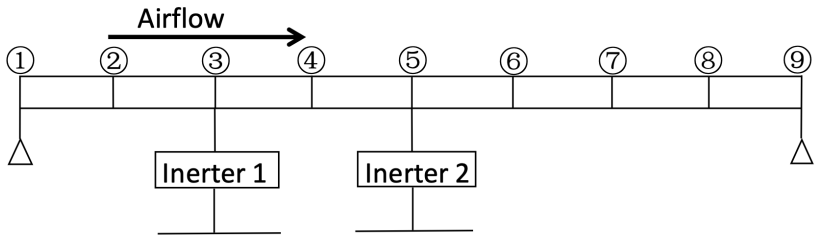

Figure 14. Schematic diagram of flutter control with 2 inerters installed at joints 3 and 5, out of 9 joints, for an 8-finite-element model.

It is observed that the best flutter control effect for the specific parameters considered can be obtained with the configuration of the effective mass ratio of inerter 1 at 0.09 and the effective mass ratio of inerter 2 at 1.89, as seen in Figure 15. Compared to the method

with one inerter, a two-inerter controlling strategy provides similar results when only considering the coalescence of flutter modes 1 and 2; however, the combined effective mass ratio of using two inerters is higher.

5.2.2. Two Inerters with Similar Effective Mass Ratio While Varying Location Joint

Two inerters, both with the same effective mass ratio, are installed in all possible joint combinations to determine which combination of joint locations provides the highest critical aerodynamic pressure. The simulation is repeated with different effective mass ratios while keeping both inerters at the same effective mass ratio. Table 3 shows a few examples with different effective mass ratios at different joint locations. The table shows that the most optimal location is to place the inerters at joints 4, 3/8 of the beam length, and 5, 1/2 of the beam length.

Increasing the effective mass ratio to the highest value in this study of 2.00 for both inerters at joints 4, 3/8 of the beam length, and 5, 1/2 of the beam length, yielded a maximum critical aerodynamic pressure parameter of 1016. Compared to the results with one inerter, this result utilizes a higher effective mass ratio of 4.00 compared to 1.53 and yields a lower critical aerodynamic pressure parameter of 1016 compared to 1271.

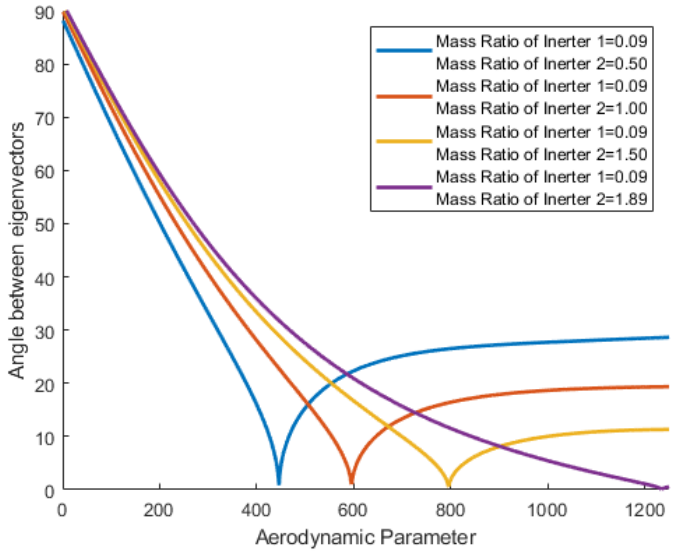

Figure 15. Angles between eigenvector for different aerodynamic pressure parameters of 2 inerters installed at joints 3 and 5.

Table 3. Inerters with the same effective mass ratio installed at different joints.

	Joints 2 and 3	**Joints 3 and 4**	**Joints 3 and 5**	**Joints 4 and 5**
Inerter 1 and 2 Effective Mass Ratio 0.10	299	326	333	361
Inerter 1 and 2 Effective Mass Ratio 0.20	300	355	350	405
Inerter 1 and 2 Effective Mass Ratio 0.20	300	355	350	405
Inerter 1 and 2 Effective Mass Ratio 0.30	311	394	364	446
Inerter 1 and 2 Effective Mass Ratio 0.40	331	446	376	485

5.2.3. Optimizing the Effective Mass Ratio at Joint Locations

One inerter was placed at joint 4, 3/8 of the beam length, and the second inerter was placed at joint 5, 1/2 of the beam length, since these locations are indicated to be the most optimal locations when using the same effective mass ratio for both inerters. The effective mass ratio in the simulations is varied independently from 0.1 to 2 in 0.1 increments to determine the highest possible aerodynamic pressure parameter that can be achieved when analyzing the coalescence of modes 1 and 2.

Figure 16 is a schematic diagram of the case with inerters installed at joints 4 and 5. The simulation results are illustrated in Figure 17, which depicts the coalescence of modes 1 and 2. Figure 18 shows the relationship between the critical aerodynamic pressure parameters and the angle between the eigenvectors of modes 1 and 2. The optimal critical aerodynamic pressure parameter value is 1271, while the respective effective mass ratios of inerter 1 and inerter 2 are 0.31 and 1.93, which can be found in Table 4. When compared to the results with one inerter, this method increases the critical aerodynamic parameter by 40. However, the sum of the effective mass ratio has a total value of 1.98, compared to 1.53 with one inerter.

Although not demonstrated, all possible combinations of mass ratios and joint locations were tested to verify that the stated combination increased the critical aerodynamic pressure to its maximum value when considering the coalescence of the two lowest modes.

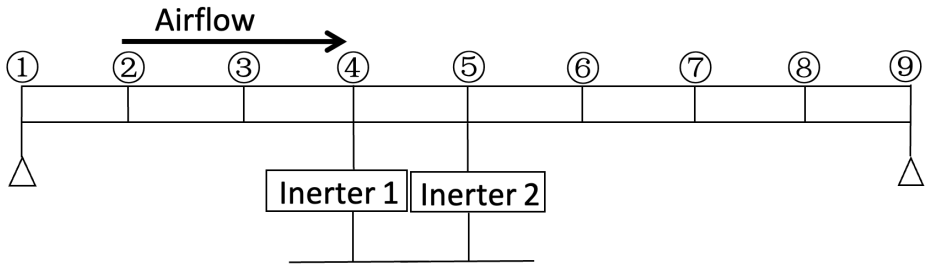

Figure 16. Schematic diagram of flutter control with 2 inerters installed at joints 4 and 5, out of 9 joints, for an 8-finite-element model.

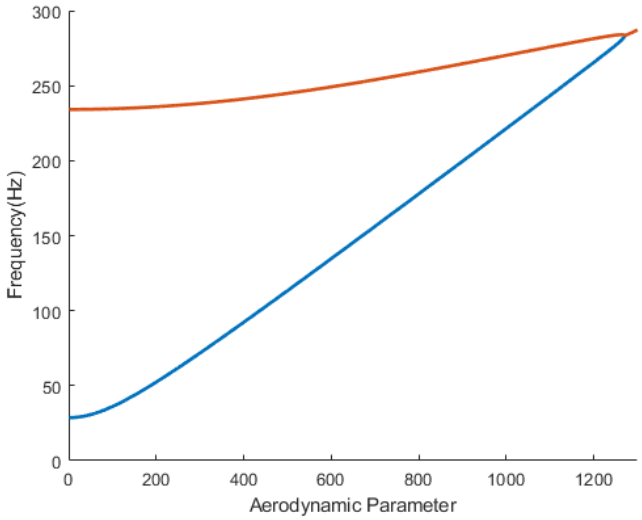

Figure 17. Critical aerodynamic pressure parameter for 2 inerters installed at joints 4 and 5 resulting from the two lowest natural frequencies coalescing.

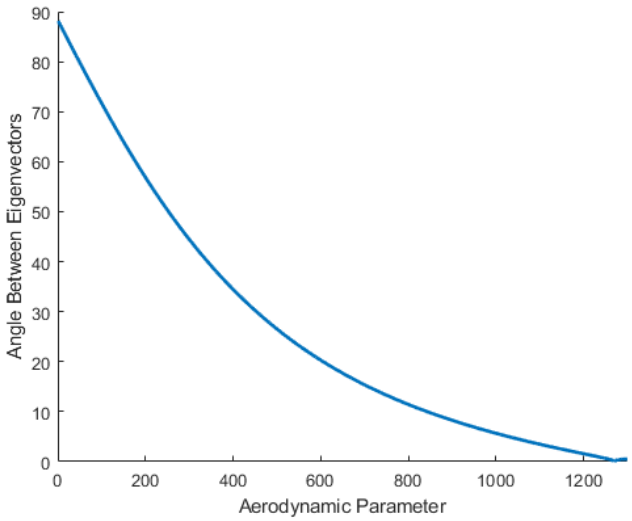

Figure 18. Angles between eigenvectors for different aerodynamic pressure parameters of 2 inerters installed at joints 4 and 5.

Table 4. Optimal critical aerodynamic pressure parameters of 2 inerters with different effective mass ratios installed at joints 4 and 5.

Effective Mass Ratio of Inerter at Joint 4	Effective Mass Ratio of Inerter at Joint 5	Critical Aerodynamic Parameter
0.31	1.93	1271

6. Concluding Remarks

An eigenvector orientation method for the flutter control of panels using an inerter is introduced in this study. To illustrate the formulation and procedure, the aeroelastic equation of motion for a panel equipped with inerters is developed using two nodes and four-degrees-of-freedom wide-beam elements to simulate panels. An effective eigenvector orientation approach is presented to detect the onset of flutter. This method can provide a lead time for flutter control, which is important and could be established by tracking the angle between the coalescing eigenvectors as it gradually approaches zero. To illustrate the concept and explore the feasibility of the application of the proposed procedure, a simple illustrative example using a two-dimensional panel (a wide beam) is chosen. For the specific examples chosen, the calculation may reveal the feasibility of application and the advantages of the current proposed method.

Two cases are simulated in order to validate the basic theory of flutter control using inerters. Results of the two cases show that the critical aerodynamic pressure parameter of flutter occurrence can be offset to a higher level through the use of inerters. The effectiveness depends on the effective mass ratio and location of the inerters. In the example of the eight-element model using only one inerter, it is seen that the optimal effectiveness can be achieved by installing the inerter at the midspan, joint 5, with an effective mass ratio of 1.53. For the two-inerter examples, there are also peak critical aerodynamic pressure parameters, which can be reached by optimizing the locations and effective mass ratios of the inerters. The optimal flutter control effectiveness can be obtained when two inerters are installed at joints 4, 3/8 of the beam length, and 5, 1/2 of the beam length, with effective mass ratios of 0.31 and 1.93, respectively.

In light of the simulation results of the present cases studied, it can be seen that the use of inerters may be promising for flutter control. Inerters can achieve a mass amplification effect without increasing the total physical mass of the aeroelastic system. Thus, the use of an inerter may be beneficial for an aeroelastic structure to achieve the design objective of

mass optimization. For a further study, it may be of interest to compare the proposed design to other design changes, such as local mass thickening. However, the next logical research step would be to design and conduct experiments on a wide beam with the proposed inerter. This next step would include considering the mass of a single inerter as an industrial and practical example, while also utilizing a range of inertance values of the inerter b, including the case where b is larger than the mass of the structure.

It is interesting to note that when using inerters, it seems that the highest possible aerodynamic parameter is 1271. Further increasing the effective mass ratio would no longer cause coalescence between the lowest modes but would cause coalescence at higher modes. In addition, the optimal location of the inerters seems to correlate with the first mode shape of a simply supported beam panel. Thus, the fundamental mode shapes may play a role when identifying where to locate the inerters, i.e., the placement of the inerters may be more effective in controlling flutter at the highest amplitude of the mode shape along the wide beam.

Although the present study has dealt with the flutter control of simply supported wide-beam panels using inerters, the method can be extended to the flutter control of more general cases with flat or curved panels using triangular and quadrilateral plate finite elements in bending. Moreover, it seems a logical next step to develop a semi-active flutter control strategy based on the inerter-based passive controlling method.

Author Contributions: Conceptualization, H.L.; Data curation, P.M.; Writing—original draft, H.L.; Writing—review & editing, P.M.; Supervision, H.T.Y.; Project administration, H.T.Y. All authors have read and agreed to the published version of the manuscript.

Funding: This research received no external funding.

Data Availability Statement: No new data were created or analyzed in this study. Data sharing is not applicable to this article.

Conflicts of Interest: The authors declare no conflict of interest.

References

1. Yang, T.Y.; Sung, S.H. Finite-Element Panel Flutter in Three-Dimensional Supersonic Unsteady Potential Flow. *AIAA J.* **1977**, *15*, 1677–1683. [CrossRef]
2. Olson, M.D. Finite Elements Applied to Panel Flutter. *AIAA J.* **1967**, *5*, 2267–2270. [CrossRef]
3. Olson, M.D. Some Flutter Solutions Using Finite Elements. *AIAA J.* **1970**, *8*, 747–752. [CrossRef]
4. Wang, Z.; Qin, X.; Yang, H.T. Active Suppression of Panel Flutter with Piezoelectric Actuators using Eigenvector Orientation Method. *J. Sound Vib.* **2012**, *331*, 1469–1482. [CrossRef]
5. Sebastijanovic, N.; Ma, T.; Yang, H.T.Y. Panel Flutter Detection and Control Using the Eigenvector Orientation Method and Piezoelectric Layers. *AIAA J.* **2007**, *45*, 118–127. [CrossRef]
6. Sebastijanovic, N.; Ma, T.; Dicarlo, A.; Yang, H.T.Y. An Eigenvector Orientation Approach for Detection and Control of Panel Flutter. In Proceedings of the Smart Structures and Materials 2005: Smart Structures and Integrated Systems, San Diego, CA, USA, 7–10 March 2005.
7. Crawley, E.F.; Luis, J.D. Use of Piezoelectric Actuators as Elements of Intelligent Structures. *AIAA J.* **1987**, *25*, 1373–1385. [CrossRef]
8. Zhou, R.C.; Lai, Z.; Xue, D.Y.; Huang, J.K.; Mei, C. Suppression of Nonlinear Panel Flutter with Piezoelectric Actuators using Finite Element Method. *AIAA J.* **1995**, *33*, 1098–1105. [CrossRef]
9. Kim, M.; Li, Q.; Huang, J.K.; Mei, C. Active Control of Nonlinear Panel Flutter Using Aeroelastic Modes and Piezoelectric Actuators. *AIAA J.* **2008**, *46*, 733–743. [CrossRef]
10. Moon, S.H.; Hwang, J.S. Panel Flutter Suppression with an Optimal Controller based on the Nonlinear Model using Piezoelectric Materials. *Compos. Struct.* **2005**, *68*, 371–379. [CrossRef]
11. Forster, E.E.; Yang, H.T.Y. Flutter Control of Wing Boxes Using Piezoelectric Actuators. *J. Aircr.* **1998**, *35*, 949–957. [CrossRef]
12. Smith, M. Synthesis of Mechanical Networks: The Inerter. *IEEE Trans. Autom. Control* **2002**, *47*, 1648–1662. [CrossRef]
13. Smith, M.C. The Inerter Concept and Its Application. In Proceedings of the Society of Instrument and Control Engineers (SICE) Annual Conference, Fukui, Japan, 4–6 August 2003.
14. Smith, M.C.; Wang, F.C. Performance Benefits in Passive Vehicle Suspensions Employing Inerters. *Veh. Syst. Dyn.* **2004**, *42*, 235–257. [CrossRef]
15. Wang, F.C.; Liao, M.K.; Liao, B.H.; Su, W.J.; Chan, H.A. The Performance Improvements of Train Suspension Systems with Mechanical Networks Employing Inerters. *Veh. Syst. Dyn.* **2009**, *47*, 805–830. [CrossRef]

16. Wang, F.C.; Liao, M.K. The Lateral Stability of Train Suspension Systems Employing Inerters. *Veh. Syst. Dyn.* **2010**, *48*, 619–643. [CrossRef]
17. Wang, F.C.; Hsieh, M.R.; Chen, H.J. Stability and Performance Analysis of a Full-Train System with Inerters. *Veh. Syst. Dyn.* **2012**, *50*, 545–571. [CrossRef]
18. Jiang, J.Z.; Matamoros-Sanchez, A.Z.; Goodall, R.M.; Smith, M.C. Passive Suspensions Incorporating Inerters for Railway Vehicles. *Veh. Syst. Dyn.* **2012**, *50*, 263–276. [CrossRef]
19. Evangelou, S.; Limebeer, D.J.N.; Sharp, R.S.; Smith, M.C. Control of Motorcycle Steering Instabilities. *IEEE Control Syst.* **2006**, *26*, 78–88.
20. Evangelou, S.; Limebeer, D.J.N.; Sharp, R.S.; Smith, M.C. Mechanical Steering Compensators for High-Performance Motorcycles. *J. Appl. Mech.* **2006**, *74*, 332–346. [CrossRef]
21. Wang, F.C.; Hong, M.F.; Chen, C.W. Building Suspensions with Inerters. *Proc. Inst. Mech. Eng. Part C J. Mech. Eng. Sci.* **2009**, *224*, 1605–1616. [CrossRef]
22. Li, H.; Yang, H.T.; Kwon, I.Y.; Ly, F.S. Bio-Inspired Passive Base Isolator with Tuned Mass Damper Inerter for Structural Control. *Smart Mater. Struct.* **2019**, *28*, 105008. [CrossRef]
23. Sun, X.Q.; Chen, L.; Wang, S.H.; Zhang, X.L.; Yang, X.F. Performance Investigation of Vehicle Suspension System with Nonlinear Ball-Screw Inerter. *Int. J. Automot. Technol.* **2016**, *17*, 399–408. [CrossRef]
24. Wang, F.C.; Hong, M.F.; Lin, T.C. Designing and Testing a Hydraulic Inerter. *Proc. Inst. Mech. Eng. Part C J. Mech. Eng. Sci.* **2010**, *225*, 66–72. [CrossRef]
25. Hodges, D.H.; Pierce, G.A. *Introduction to Structural Dynamics and Aeroelasticity*; Cambridge University Press: Cambridge, UK, 2002.
26. Dowel, E.H. *Panel Flutter (NASA Space Vehicle Design Criteria (Structures))*; NASA SP-8007; NASA Langley Research Center: Hampton, VA, USA, 1972.
27. Alder, M. Development and Validation of a Fluid–Structure Solver for Transonic Panel Flutter. *AIAA J.* **2015**, *53*, 3509–3521. [CrossRef]
28. Pidaparti, R.M.V.; Yang, H.T.Y. Supersonic Flutter Analysis of Composite Plates and Shells. *AIAA J.* **1993**, *31*, 1109–1117. [CrossRef]
29. Yang, T.Y. *Finite Element Structural Analysis*; Prentice-Hall: Hoboken, NJ, USA, 1986.
30. Sun, Q.; Xing, Y. Exact Eigensolutions for Flutter of Two-Dimensional Symmetric Cross-Ply Composite Laminates at High Supersonic Speeds. *Compos. Struct.* **2018**, *183*, 358–370. [CrossRef]
31. Afolabi, D.; Pidaparti, R.M.V.; Yang, H.T.Y. Flutter Prediction Using an Eigenvector Orientation Approach. *AIAA J.* **1998**, *36*, 69–74. [CrossRef]
32. Mccall, J. Genetic Algorithms for Modelling and Optimisation. *J. Comput. Appl. Math.* **2005**, *184*, 205–222. [CrossRef]